Cell, Vol. 102, 625–633, September 1, 2000, Copyright ©2000 by Cell Press

Structural Basis for Relief of Autoinhibition of the Dbl Homology Domain of Proto-Oncogene Vav by Tyrosine Phosphorylation

Behzad Aghazadeh,*† William E. Lowry,‡ Xin-Yun Huang,† and Michael K. Rosen*§‖

*Cellular Biochemistry and Biophysics Program
Memorial Sloan-Kettering Cancer Center
New York, New York 10021

†Graduate Program in Physiology and Biophysics

‡Graduate Program in Neuroscience

§Graduate Program in Biochemistry and Structural Biology
Weill Graduate School of Medical Sciences
Cornell University
New York, New York 10021

Summary

Rho-family GTPases transduce signals from receptors leading to changes in cell shape and motility, mitogenesis, and development. Proteins containing the Dbl homology (DH) domain are responsible for activating Rho GTPases by catalyzing the exchange of GDP for GTP. Receptor-initiated stimulation of Dbl protein Vav exchange activity involves tyrosine phosphorylation. We show through structure determination that the mVav1 DH domain is autoinhibited by an N-terminal extension, which lies in the GTPase interaction site. This extension contains the Tyr174 Src-family kinase recognition site, and phosphorylation or truncation of this peptide results in stimulation of GEF activity. NMR spectroscopy data show that the N-terminal peptide is released from the DH domain and becomes unstructured upon phosphorylation. Thus, tyrosine phosphorylation relieves autoinhibition by exposing the GTPase interaction surface of the DH domain, which is obligatory for Vav activation.

Introduction

Members of the Ras superfamily of GTPases regulate a diverse array of intracellular signaling pathways required for normal and transformed cell growth. These proteins act as molecular switches by cycling between active GTP-bound and inactive GDP-bound states. Two classes of proteins accelerate their low intrinsic rate of nucleotide cycling: GTPase activating proteins (GAPs) catalyze the hydrolysis of the terminal phosphate group of the bound nucleotide to render the GTPases inactive, whereas guanine nucleotide exchange factors (GEFs) promote acquisition of the active state by accelerating the exchange of GDP for GTP. Structural differences associated with the two nucleotide states allow GTPases to selectively target downstream effectors when activated (Bourne et al., 1991; Boguski and McCormick, 1993).

The Rho-family GTPases, Rho, Rac, and Cdc42, are primarily known as regulators of the actin cytoskeleton. Each member is capable of promoting distinct actin-based cytoskeletal structures required for cell adhesion and motility in morphogenic, chemotactic, and profilerative responses (Hall, 1998). These GTPases also control cell growth and apoptosis through activation of the extracellular signal–regulated kinase (ERK) and c-Jun N-terminal kinase (JNK) cascades (Hall, 1998; Chen and Tan, 2000). Deregulation of these signaling pathways can lead to disease processes such as tumorigenesis (Qiu et al., 1995) and developmental disorders (Pasteris et al., 1994; Billuart et al., 1998; Ambruso et al., 2000).

Rho-GTPases are activated by GEFs that contain a conserved region termed the Dbl homology (DH) domain that is responsible for catalyzing the nucleotide exchange (Cerione and Zheng, 1996). In contrast to the Ras-GEF Sos, which appears to be activated largely through receptor-mediated translocation to cell membranes (where the GTPase resides [Downward, 1996]) the mechanisms whereby upstream signals are relayed to the Dbl GEFs are poorly understood. While activation of these proteins also involves cellular targeting, other regulatory mechanisms are clearly important as well (Cerione and Zheng, 1996). The significance of DH domain regulation is evidenced by involvement in diseases. Indeed, many members of the Dbl family GEFs were initially identified based on their oncogenic potential (Cerione and Zheng, 1996), or have been directly linked to developmental disorders (Pasteris et al., 1994) and tumor metastasis (Michiels et al., 1995).

One of the best characterized Rho-GEF proteins is the proto-oncogene product, Vav. This protein is essential for cytoskeletal, proliferative, and apoptotic pathways in lymphoid cell development and signaling responses. B and T lymphocytes derived from Vav −/− mice show defective antigen receptor induced proliferation (Fischer et al., 1995; Tarakhovsky et al., 1995; Zhang et al., 1995) and F-actin polymerization (Fischer et al., 1998; Holsinger et al., 1998). Stimulation of Vav results in Rac-mediated formation of lamellipodia and activation of JNK in vivo (Crespo et al., 1996), and Vav GEF activity is specific for Rac in vitro (Crespo et al., 1997).

Vav and its homologs, Vav2 and Vav3, are composed of an N-terminal calponin homology (CH) domain (residues 1–116) followed by an acidic region (Ac) (132–176), the DH (185–375) and PH (pleckstrin homology) (398–508) domains common to all Rho GEFs, a zinc finger (ZF) (516–565) domain, a short proline-rich region (PR) (607–610), and an SH3-SH2-SH3 (612–844) module at the C terminus (Bustelo, 1996). Interactions between different regions of Vav are involved in regulating the GEF activity of the DH domain. Vav becomes rapidly phosphorylated in response to antigen stimulation of the B- and T-cell receptors (Bustelo and Barbacid, 1992; Bustelo et al., 1992; Margolis et al., 1995) through the action of Syk and Src-family tyrosine kinases (Deckert et al., 1996; Han et al., 1997). This phosphorylation event results in the stimulation of nucleotide exchange activity (Crespo et al., 1997). Although there is evidence of additional phospho-tyrosine residues regulating GEF activity, the best characterized are three conserved sites in

‖To whom correspondence should be addressed (e-mail: rosen@mrnmr1.mskcc.org).

the Ac region. Of these, Tyr174 is the most extensively studied and has been shown to be a substrate for Syk and the Src-family tyrosine kinase, Lck (Brunati et al., 1995; Han et al., 1997). Phosphorylation of this residue enhances GEF activity in vitro (Han et al., 1997) and truncation of the N-terminal 186 residues (Δ1–186) leads to phosphorylation independent activation of Vav2 GEF function (Schuebel et al., 1998). Compared to Vav molecules containing Tyr174, Vav (Δ1–186) is up to 100-fold more potent in focus formation assays when transfected into NIH 3T3 cells (Abe et al., 1999). Mutation of Tyr174 to phenylalanine also potentiates DH mediated transformation (Lopez-Lago et al., 2000). In contrast, Tyr→Phe mutations at the other N-terminal phosphorylation sites (Tyr142 and Tyr160) (Lopez-Lago et al., 2000) and truncations of Vav at residues 127 or 168 (Abe et al., 1999), increase the oncogenic potential to a lesser degree, implicating Tyr174 as a key regulatory site. Taken together, these data imply that the N terminus of Vav is autoinhibitory and phosphorylation of Tyr174 relieves this negative regulation.

In this study, we have determined the solution structure of the autoinhibited Vav DH domain (residues 170–375) and characterized its structural changes on phosphorylation at Tyr174. The conserved portion of the domain (residues 186–375) is architecturally similar to other members of the Dbl family. The N-terminal autoinhibitory extension forms an α helix that binds in the DH domain active site through contacts to conserved residues, blocking access to GTPases. Tyr174 forms an integral part of this autoinhibitory interface, and is largely buried in the intramolecular complex. Phosphorylation of Tyr174, or removal of the N-terminal peptide greatly enhances the DH domain exchange activity. NMR spectroscopic data show that phosphorylation of Tyr174 causes the N-terminal peptide to become unstructured and release from the DH domain. Thus, the Vav DH domain is activated through phosphorylation-mediated exposure of the active site.

Results

To understand the mechanism of Vav DH domain activation, we examined several Vav constructs for their ability to stimulate nucleotide exchange on Rac and Cdc42. Based on sequence comparisons with DH domains of known structure (Aghazadeh et al., 1998; Liu et al., 1998; Soisson et al., 1998), we expressed and purified residues 181–375 of mouse Vav1 comprising the isolated DH fragment. GDP release assays show that this fragment is active toward Rac1 (Figure 1). In agreement with previous findings, no GEF activity was observed toward Cdc42 under the same conditions (Figure 1). In contrast, purified Vav170–375 containing the Tyr174 phosphorylation site was inactive toward both Rac1 and Cdc42 (Figure 1). Activity toward Rac1 but not Cdc42 was restored to levels comparable to Vav181–375 through preincubation with Src tyrosine kinase under conditions leading to stoichiometric conversion of Vav to a single phosphorylated species (see below). Kinase assays measuring ^{32}P incorporation showed that Vav170–375, but not Vav181–375, was phosphorylated by Src kinase (Figure 1, insert). Thus, in the absence of other regions of the molecule, the Vav DH domain is both active and capable of exerting GTPase selectivity, and Tyr174 functions as the main regulatory site of GEF activity.

Structure Determination

To better understand the mechanism of inhibition by the N-terminal extension, we determined the solution structure of Vav170–375 by NMR spectroscopy. Structure determination of this 24 kDa fragment required utilization of recently developed isotopic labeling, spectroscopic, and computational methodologies. Sequential assignments were obtained from a selectively methyl-protonated (Leu, Val, and Ile [δ1 only]), otherwise $^{2}H/^{15}N/^{13}C$-labeled sample, using heteronuclear three-dimensional NMR experiments designed specifically for deuterated systems (see Experimental Procedures). Methyl resonances were obtained from methyl-optimized HCCTOCSY-NNH and CCC-TOCSY-NNH NMR experiments (Gardner et al., 1996). Aromatic ring proton assignments were obtained using 2D TOCSY and NOESY experiments (Wuthrich, 1986) performed on a selectively methyl-protonated, otherwise deuterated sample with the additional labeling of $^{1}H/^{12}C/^{14}N$ at the Tyr and Phe positions. The remaining side chain resonances were assigned from standard NMR experiments on a $^{13}C/^{15}N/^{1}H$-labeled sample. The use of deuteration in conjunction with selective protonation of residues forming the hydrophobic core allowed us to acquire a series of three- and four-dimensional NOESY experiments that were used in the initial protein global fold determination. In particular, the favorable relaxation properties of the selectively methyl- and aromatic-protonated sample allowed us to obtain critical NOEs between these functional groups using the constant time $^{1}H/^{13}C_{methyl}/^{1}H_{aromatic}$ NOESY experiment (modified from Zwahlen et al., 1998). The high-resolution structure was subsequently obtained using ARIA for automated assignment of ^{15}N- and ^{13}C-edited NOESY experiments (Nilges et al., 1997).

Structure of the Vav DH Domain and Mechanism of Autoinhibition

The structure of Vav170–375 was calculated from a total of 3432 NMR distance restraints (Table 1). In addition, 326 chemical shift–based backbone torsion angle restraints obtained from the program TALOS were included (Cornilescu et al., 1999), as were 79 side chain torsion restraints. Figure 2 shows a backbone superposition of the 20 lowest energy structures. Residues 178–198 are disordered due to a lack of NOEs observed for this region. The root mean square deviation for the structured regions (residues 170–177 and 199–375) is 0.63 Å for backbone and 1.12 Å for all heavy atoms (Table 1).

The Vav DH domain is structurally similar to previously reported DH domains (Aghazadeh et al., 1998; Liu et al., 1998; Soisson et al., 1998). It is composed of 11 α helices that form a flattened, elongated bundle, giving rise to two surfaces formed by helices D, E, F, and G and A, I, J, and K (Figure 3A). The latter has been identified as the GTPase interaction site (Liu et al., 1998) and many of the residues required for GEF activity cluster on this surface. These include the exposed amino acids corresponding to Glu201 and Thr205 on helix A, Gln331,

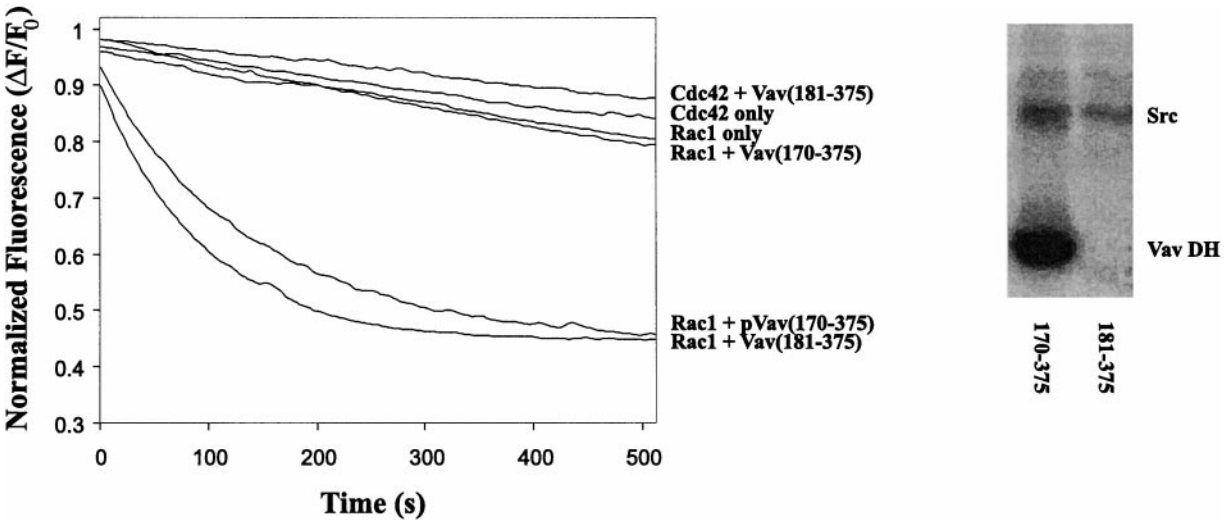

Figure 1. Rac1 and Cdc42 Nucleotide Exchange Catalyzed by Vav DH Domain Constructs

Normalized change in fluorescence (*F*) of (mant-GDP)-Cdc42 and Rac1 complex on addition of Vav170–375, Vav181–375, and phosphorylated Vav170–375. The amount of Mant-GDP bound to the GTPase prior to GEF addition was defined as 100% GDP bound. Insert: phosphorylation of Vav170–375 but not Vav181–375 by Src kinase.

Lys335 and Leu338 on helix J, Asn371 and Glu372 on helix K (Aghazadeh et al., 1998) in Vav, which are conserved in sequence as well as the relative orientation of their side-chains. It seems therefore that structurally the DH domain of Vav has potential for robust exchange activity. The N-terminal eight residues (170–177) containing the IY(174)EDL phosphorylation motif form an additional α helix attached by a flexible linker (residues 178–198) to the N terminus of the DH domain fold. This element packs orthogonally to helices A and I across the center of the active site (Figure 3A). Side chains of residues Ile173, Tyr174, and Leu177 make contacts to a hydrophobic patch created by Tyr209 and Thr212 (helix A), Phe320 (H-I loop), and Leu325 and Val328 (helix I) of the DH domain (Figure 3B). NOEs from the N-terminal peptide to Phe320 result in elevation of the C terminus

Table 1. Statistics for the Ensemble of 20 NMR Derived Structures

Restraints for structure calculation[a]	
Total restraints	3966
Total NOE restraints	3523
Unambiguous	2212
Ambiguous	1215
Hbonds	96
Dihedral (Φ, Ψ, χ^1, χ^2)	182, 182, 55, 24
Statistics for structure calculation[b]	
rmsd from experimental restraints	
Distance (Å)	0.0015 ± 0.0001
Angles (°)	0.34 ± 0.01
Final Energies (kcal mol^{-1})	
E_{total}	198 ± 27
E_{NOE}	38 ± 15
E_{cdih}	4 ± 3
Coordinate precision[c]	(residues 170–177, 199–208)
rmsd of backbone atoms (N, Cα, C′)	0.63 Å ± 0.09
rmsd of all heavy atoms	1.12 Å ± 0.06
Procheck analysis	
Most favored	84.3%
Additional allowed	13.8%
Generously allowed	1.4%
Disallowed region	0.4%

[a] The final values for the force constants employed for the various terms in the target function employed for simulated annealing are as follows: 5 kcal mol^{-1}Å^{-4} for the quartic van der Waals repulsion term (with van der Waals radii set to 0.78 times their value defined in the paramallhdg-pro parameter set), 50 kcal mol^{-1}Å^{-2} for the experimental distance restraints, 200 kcal mol^{-1}rad^{-2} for the experimental torsion angle restraints.
[b] None of the final structures have distance restraint violations greater than 0.3 Å or dihedral violations greater than 5°.
[c] Defined as average root-mean-squared difference for the stated residues between the final 20 structures and the average coordinates.

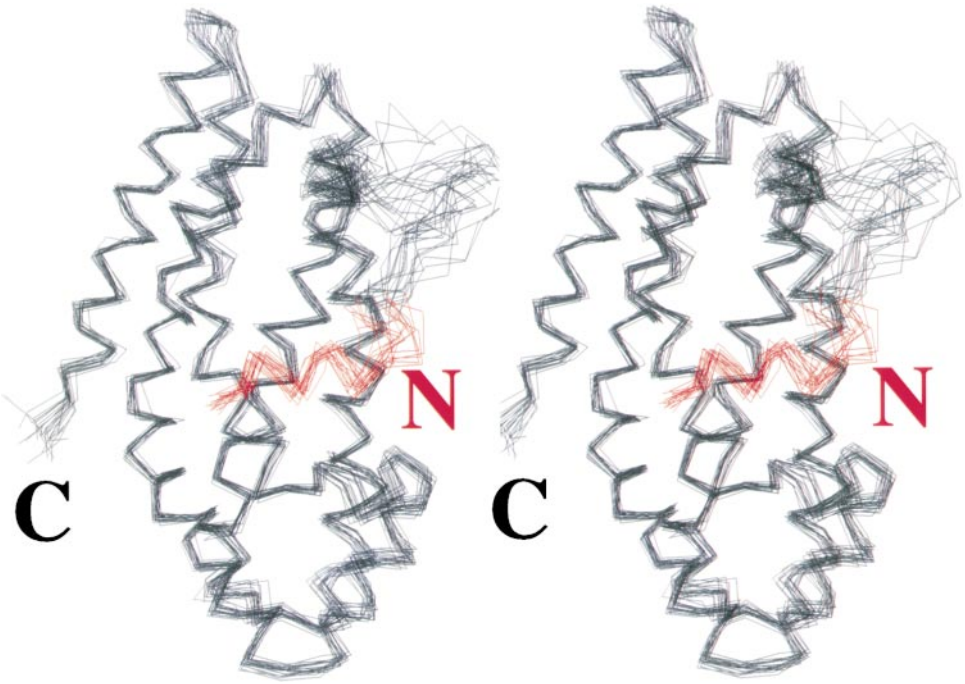

Figure 2. Stereoview of the Backbone (N, Cα, and C′) of 20 superimposed structures of Vav170–375
Residues 170–180 containing the Tyr174 phosphorylation motif are red, and residues 181–375 are black.

of helix H by ~12 Å in our calculations compared to other known DH domain structures. Interestingly, side chains of residues corresponding to Phe320, Leu325, and Val328 are exposed in DH domains of both PIX and mSos (Aghazadeh et al., 1998; Soisson et al., 1998), but are buried under the autoinhibitory helix in the Vav structure. Moreover, in Trio, most DH domain residues indicated in the interaction with Rac (Liu et al., 1998) map to regions immediately adjacent to the autoinhibitory contacts in our structure. In particular, the backbone $^{1}H/^{15}N$-HSQC resonance of Arg1369 in Trio (corresponding to Arg332 in Vav) is affected by the titration of Rac1, and mutagenesis data have shown that this residue is critical for GEF function (Liu et al., 1998). In our structure, the guanidinium group of Arg332, which forms a conserved, buried salt bridge with Glu206, appears to stabilize the Tyr174 hydroxyl group, which is directed toward the hydrophobic core of the DH domain (Figure 3B). Finally, in Dbl, mutagenesis of the conserved glutamine corresponding to Gln331 in Vav, which is buried by the first turn of the autoinhibitory helix in our structure, eliminates GEF activity (Zhu et al., 2000). We therefore conclude that Vav GEF function is inhibited through the occlusion of residues important for GTPase binding and nucleotide exchange catalysis. The tyrosine phosphorylation motif, I/VYXXL/I, which forms the autoinhibitory helix, is conserved throughout the Vav proteins, indicating that this mechanism of regulation is conserved among this family of GEFs.

Mechanism of Activation by Tyr174 Phosphorylation

We next investigated the structural changes that occur upon phosphorylation resulting in the activation of the Vav DH domain. We were able to phosphorylate a sample of $^{15}N/^{13}C$-labeled Vav170–375 to a high degree (>90%), yielding a single species as monitored through changes of $^{1}H/^{15}N$ and $^{1}H/^{13}C$ correlation spectra (Figure 4A). The majority of signals in the phosphorylated and unphosphorylated spectra are similar, indicating no gross structural changes in the body of the domain. However, changes were observed for the methyl groups comprising the inhibitory binding pocket (Ile173, Leu177, Leu325, and Val328) (Figure 4A). In addition, a number of new resonances appeared in the $^{1}H/^{15}N$ HSQC spectrum (Figure 4B). These have much higher intensities compared to the rest of the spectrum while showing poor chemical shift dispersion in the proton dimension, indicative of an unstructured and mobile region. Sequential assignment has mapped these signals to the N-terminal 14 residues of Vav170–375. Chemical shift index (CSI) analysis (Wishart and Sykes, 1994) verified that these residues lack secondary structure in solution in the phosphorylated state. We therefore conclude that phosphorylation of Tyr174 causes release of the N-terminal inhibitory arm from the body of the DH domain, exposing the GEF active site. Disruption of inhibitory contacts appears to be caused by a combination of steric clashes between Tyr174 phosphate group and the side chains of Arg332 and Tyr209 (Figure 3B), and the energetic cost of desolvating the phosphate upon introduction into the binding pocket. Phosphorylation of threonine residues has also been shown to destabilize helices (Szilak et al., 1997). It is possible that an analogous disruption of the inhibitory helix by Tyr174 phosphorylation also contributes to the weakening of contacts between Ile173 and Leu177 and residues Phe320 and Leu325 of the DH body.

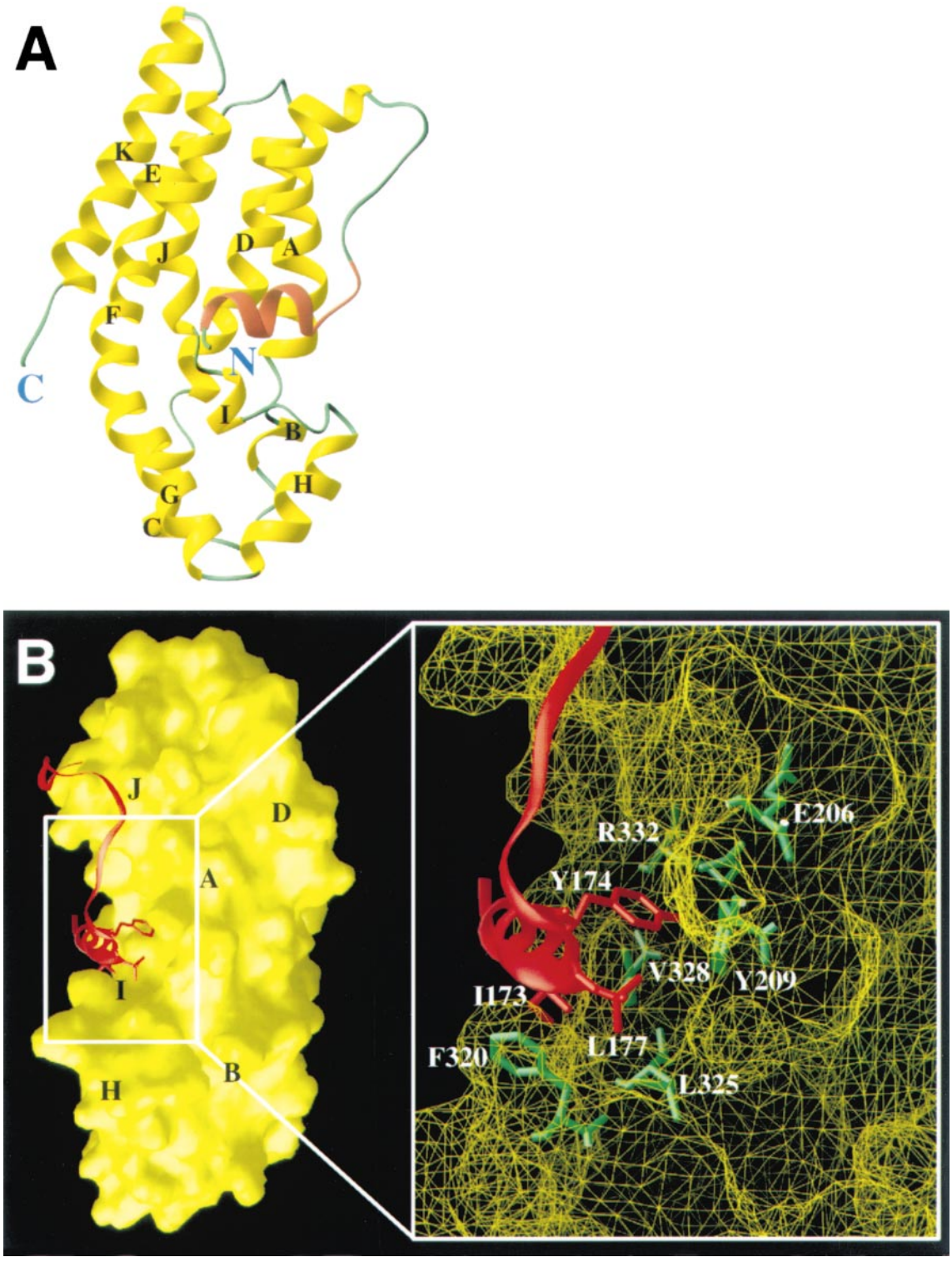

Figure 3. Structure of the Autoinhibited Vav170–375

(A) Ribbons (Carson, 1991) depiction of a representative confomer from the final ensemble of Vav DH domain structures. Residues 170–180 encompassing the inhibitory helix are red, 181–375 are yellow, loops are green.

(B) Autoinhibited DH domain, rotated ~90° about a vertical axis with respect to 3A. Left: a yellow molecular surface of the DH domain (residues 195–375) with the N-terminal autoinhibitory arm (residues 170–194) depicted as a red ribbon. Right: indicated expansion of the binding site of the inhibitory helix on the DH domain. Residues involved in the interaction are colored green on the DH domain and red on the inhibitory helix. Molecular surfaces of the DH domain represented as a yellow net. Figure produced with GRASP (Nicholls et al., 1991).

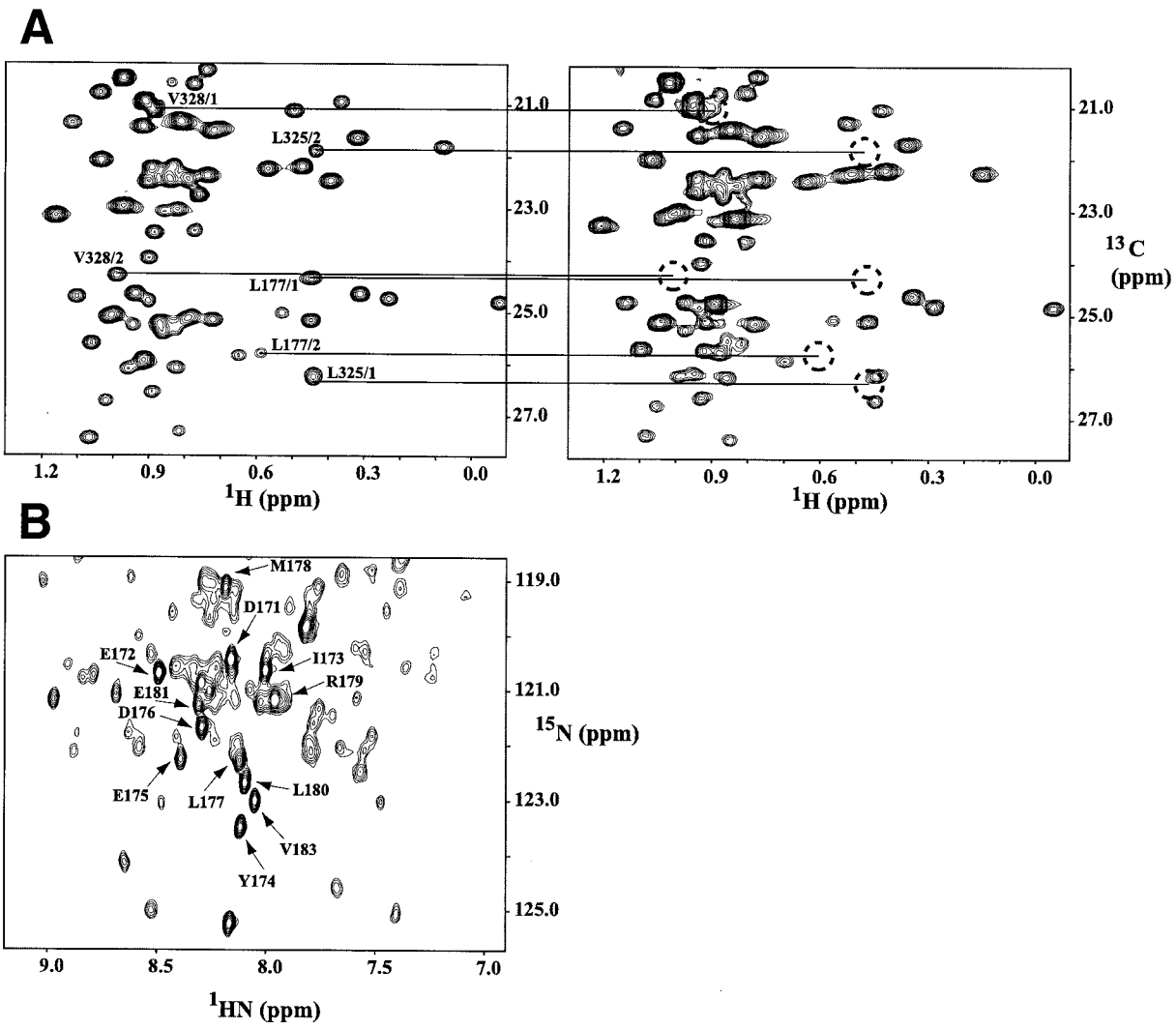

Figure 4. Correlation Spectra of Phosphorylated and Unphosphorylated Vav170–375

(A) Leu/Val methyl region of $^{1}H/^{13}C$ constant-time HSQC spectrum acquired on selectively methyl labeled samples (see text) of Vav170–375 (left panel) and phosphorylated Vav170–375 (right panel). Assignment of peaks shifted upon phosphorylation are shown.

(B) Region of $^{1}H/^{15}N$-HSQC spectrum of phosphorylated Vav. Assignment of intense peaks appearing upon phosphorylation are shown. Resonances of Gly170 and Ser182 do not fall within the displayed region.

Discussion

Phosphorylation of Dbl proteins occurs in response to stimulation of many signaling pathways, and often correlates with Rho protein activation in vivo. Consistent with this, numerous kinases are known to play prominent roles in Rho GTPase-mediated processes, such as cell adhesion and spreading, focal adhesion disassembly, and migration (Thomas and Brugge, 1997). In several cases, phosphorylation has been shown to directly increase GEF activity in vitro (Crespo et al., 1997; Fleming et al., 1999; Kiyono et al., 2000). Therefore, tyrosine phosphorylation–dependent activation of Rho-GEFs may be a general mechanism for stimulation of Rho GTPase responses. The best studied Rho-GEF that is activated by tyrosine phosphorylation both in vivo and in vitro, is the Vav proto-oncogene. Src- and Syk-family tyrosine kinases can activate the Vav DH domain through phosphorylation at Tyr174 (Crespo et al., 1997; Schuebel et al., 1998). Interestingly, this covalent modification can be facilitated by binding of PIP_3 to the PH domain, or alternatively hindered by PIP_2 (Han et al., 1998). These interactions correlate with the binding of the PH domain to a DH construct (residues 173–436), with PIP_2 enhancing, and PIP3 decreasing, the affinity (Das et al., 2000). This indicates that the Tyr174 phosphorylation site and the PH domain are thermodynamically, and possibly structurally, coupled through phospholipids. The simplest model to account for this data that is consistent with our autoinhibitory structure is shown in Figure 5, where the Tyr174 phosphorylation motif forms part of the interface between the PH and DH domains. Alternate models that do not involve direct contacts between the inhibitory helix and the PH domain are also possible, but would require more complicated means of communication between these elements. The

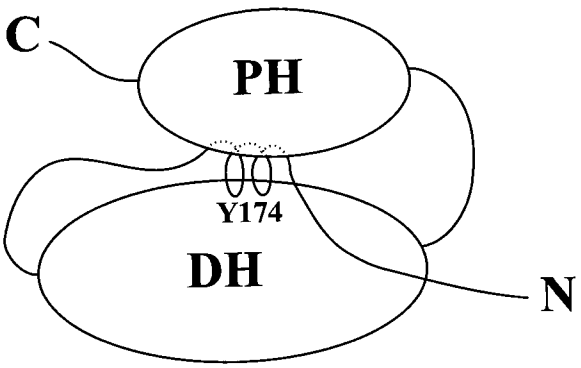

Figure 5. Model of Vav DH Domain Autoinhibition by Tyr174 Src Recognition Motif and PH Domain

structural and thermodynamic model leads to a signaling cascade for Vav activation that is initiated by the binding of PIP_3 to the PH domain. This causes the disruption of PH domain interactions with the autoinhibited DH domain and allows access of Src-family kinases to Tyr174. Subsequent phosphorylation releases the Tyr174 autoinhibitory helix region and results in the exposure of the DH active site.

A number of additional tyrosine phosphorylation sites on Vav have also been identified. However, the roles of these in regulating GEF activity remain unclear. The N-terminal Lck/Syk phosphorylation sites Tyr142 and Tyr160 have, like Tyr174, also been proposed to serve an autoinhibitory function, based on observations that truncations at positions 127, 168, and 186 increasingly potentiate Vav transformation activity (Abe et al., 1999). Interestingly, all three sites contain the sequence motif ϕYXXϕ (where ϕ = Ile, Leu, or Val, and X = hydrophilic, often acidic), observed in the case of Tyr174 to form an amphipathic helix lying in the GEF active site. This sequence is also known, in phosphorylated form, to be a consensus binding motif for Src-family kinase SH2 domains (Songyang et al., 1993). The intervening sequences between each of the sites and the DH domain are extremely hydrophilic, and unlikely to form discrete structures. Thus, it is possible that the ϕYXXϕ motifs at Tyr142 and Tyr160 can also bind, likely with lower affinity than the Tyr174 motif, in inhibitory fashion to the GEF active site. This semi-equivalence suggests that in the full-length protein, phosphorylation of all three sites may be necessary to obtain maximal GEF activity, and provides a mechanism to achieve graded activity depending on the level of kinase signaling. Repeated use of the ϕYXXϕ motif may also facilitate efficient relief of autoinhibition in vivo. Initial phosphorylation at one exposed site could position the kinase, through SH2 domain interactions, for enhanced capture of Tyr174 as it stochastically dissociates from the DH domain under thermodynamic control. Sequential processes involving initial contact with an accessible site, followed by binding or modification of a less accessible regulatory site may be a common feature of kinetic pathways leading to relief of autoinhibition.

Vav can also be phosphorylated at C-terminal sites in vivo. Like the N-terminal sites, these may be involved in intracellular targeting of the parent molecule or in recruiting other factors involved in the signaling pathway. Alternately, these sites could exert direct regulatory control over DH activity similar to Tyr174 or the PH domain. Moreover, the multiple modes of DH domain regulation may be the means through which additional specificity is achieved. Thus, to stimulate Vav GEF activity, concurrent activation of PI 3-kinase as well as Src or Syk family kinases is required. Along with the intrinsic GEF specificity for Rac, this restricts the spatial and temporal signaling through Vav in the cell.

The picture emerging from Vav activation in vivo is complex and involves an intricate network of autoregulatory units. The structure of the autoinhibited Vav DH domain is the first step in gaining structural insight into how cells elicit different responses depending on localization and collection of signals received at any given moment.

Experimental Procedures

Molecular Biology

Fragments spanning residues 170–375 and 181–375 of mVav1 were amplified from full-length cDNA by PCR, subcloned into pET11a expression vector (Novagen), and transformed into *E. coli* strain BL21(DE3). Uniform ^{15}N and ^{13}C labeling was obtained by growing cells in minimal media supplemented with $^{15}NH_4Cl$ and/or $^{13}C_6$-glucose as the sole nitrogen and carbon sources, respectively. Full deuteration at all proton positions was obtained by growing cells in 100% D_2O media supplemented with $^{13}C_6{}^2H_7$-glucose (Cambridge Isotope Laboratories) as the sole carbon source. Selective protonation at methyl positions of leucine, valine, and isoleucine was obtained as described (Gardner and Kay, 1997) by addition of 70 mg/liter of $^{13}C,^{15}N,2\text{-}^2H$ (50%),3-^2H valine (Cambridge Isotope Laboratories) and ~40 mg/liter $^{13}C,3\text{-}^2H_2$ α-ketobutyrate to fully deuterated media 30 min before induction. Similarly, addition of 50 mg/liter unlabeled protonated tyrosine and phenylalanine lead to the protonation of the side chains of these aromatics. Cells were grown at 37°C to an optical density of 0.8 at 600 nm. Protein expression was induced with 1 mM isopropyl-D-thiogalactoside for 12 hr at 25°C (H_2O growths) or 6 hr at 37°C (100% deuterated media). Protein was purified from bacterial lysate by anion exchange (Pharmacia DEAE-CL6B) and gel filtration (Pharmacia Superdex-75) chromatographies. NMR samples contained ~1.4 mM protein in 20 mM phosphate buffer (pH 7), 50 mM NaCl, 2 mM DTT, and 0.1% NaN_3. Phosphorylation reactions were performed by coincubating purified Vav proteins and Src tyrosine kinase in a molar ratio of 50:1 in the presence of excess ATP for 30 min at 30°C in 20 mM HEPES (pH 7), 50 mM NaCl, and 2 mM $MgCl_2$. Phosphorylation reactions were monitored for ^{32}P incorporation by SDS-PAGE and autoradiography. Purified Src was a gift from Yong-Chao Ma in the Huang laboratory.

Nucleotide Exchange Assays

Rac or Cdc42 were preloaded with Mant-GDP (Molecular Probes) by incubation with the fluorescent labeled nucleotide in the presence of excess EDTA as described (Nomanbhoy et al., 1996). The reaction was quenched by adding excess $MgCl_2$, and unbound nucleotide extracted using buffer exchange columns (Pharmacia). Ten nanograms of GTPase loaded with Mant-GDP was incubated in a buffer containing 20 mM HEPES (pH 7), 50 mM NaCl, and 2 mM $MgCl_2$ at 25°C. To initiate Vav-induced Mant-GDP/GDP exchange, 500 ng exchange factor was added together with 2.1 μM GDP. The time course of fluorescence was monitored using a Fluoromax-II spectrofluorometer with $\lambda_{excitation}$ at 350 nm and $\lambda_{emission}$ at 440 nm.

NMR Spectroscopy

NMR experiments were carried out at 25°C on a Varian Innova 600 MHz spectrometer equipped with 4 channels and pulsed field gradients. Data were processed using NMRpipe (Delaglio et al., 1995) and analyzed with NMRview software packages (Johnson and Blevins, 1994). Backbone ^1HN, ^{15}N, $^{13}C\alpha$, $^{13}C\beta$, and ^{13}CO assignments were

obtained for the DH domain through the following ^{2}H-decoupled, triple resonance spectra applied to a $^{2}H/^{15}N/^{13}C$-labeled sample: CT-HNCa, CT-HN(CO)Ca, HN(Ca)Cb, HN(COCa)Cb (Muhandiram and Kay, 1994), HNCO (Kay et al., 1990; Kay et al., 1994; Muhandiram and Kay, 1994), and HN(Ca)CO (Matsuo et al., 1996). Side chain resonances were assigned on a fully protonated sample through HCCH-TOCSY (Kay et al., 1993), CCC-TOCSY-NNH and HCC-TOCSY-NNH (Logan et al., 1993) experiments. All leucine, valine, and isoleucine (δ) methyl ^{1}H and ^{13}C assignments were obtained using the selectively methyl/aromatic protonated sample described in the text using optimized versions of the HCC- and CCC-TOCSY-NNH experiments (Gardner et al., 1996). All Phe and Tyr aromatic proton assignments were obtained through homonuclear ^{1}H-^{1}H TOCSY and NOESY experiments applied to the same sample.

The following NOESY spectra were recorded on the selectively methyl/aromatic protonated sample and used to generate distance restraints for structure calculation: 3D ^{15}N-edited NOESY (40 ms, 70 ms mixing time; ^{15}N-labeled sample); 3D ^{13}C-edited NOESY (75 ms); 3D constant time ^{13}C-edited NOESY (175 ms), 2D ^{1}H NOESY (150 ms), 4D $^{13}C/^{13}C$ edited NOESY (175 ms), 4D $^{15}N/^{15}N$-edited NOESY (175 ms), and 4D $^{13}C/^{15}N$ edited NOESY (175 ms).

A total of 55 $\chi 1$ ($\pm 20°-40°$) and 24 $\chi 2$ dihedral restraints ($\pm 40°$, Leu residues only) were identified based on patterns of intraresidue and sequential NOEs in the ^{15}N- and ^{13}C-edited NOESY spectra. Stereospecific assignments of valine and leucine methyl groups were obtained from a CT-$^{1}H/^{13}C$ HSQC spectrum of a 10% ^{13}C-labeled sample (Neri et al., 1989).

Structure Calculations

Initial structures were calculated using a standard torsion angle simulated annealing dynamics protocol implemented in the program CNS version 0.3 (Brunger et al., 1998). Distance restraints in these calculations were obtained from the 4D $^{13}C/^{15}N$-, 4D $^{13}C/^{13}C$- and 4D $^{15}N/^{15}N$-edited NOESY experiments and the 3D CT methyl edited experiments as described in the text. Restraints were classified as strong (1.8–2.7 Å, 2.9 Å for amides) medium (1.8–3.5 Å) and weak (1.8–5.0 Å). An additional 0.5 Å was added to the upper bound for all methyl groups. A total of 182 ϕ and 182 ψ dihedral restraints obtained from chemical shift analysis by the program TALOS (Cornilescu et al., 1999), as well as 96 hydrogen bond restraints determined from deuterium exchange experiments were included. Converged structures from the CNS calculations were then used as input to ARIA (Nilges et al., 1997), which was subsequently utilized for the iterative automated assignment of all spectra and refinement of the structures using X-PLOR (version 3.851) (Brunger et al., 1998). Tolerances for the automated assignment of NOE peaks in ARIA were set to 0.03 ppm in indirect and acquisition proton and 0.3 ppm in heteroatom dimension for all spectra. Peaks in severely overlapped regions of the spectra were not included to avoid false assignments due to incorrect positioning of these peaks. Fifteen structures were calculated in each iteration. The iterative assignment of NOEs was based on twelve structures with the lowest number of violations calculated in the preceding iteration. An assignment was included if it could be satisfied in at least 50% of the structures. The cutoff value of an ambiguous assignment was reduced progressively from 0.99 for the first iteration to 0.85 in iteration 6. After each iteration, structures obtained were analyzed to ensure that none of the restraints utilized in the initial CNS calculations were violated. Final structures were evaluated using the program ProcheckNMR (Laskowski et al., 1996).

Acknowledgments

We thank Yong-Chao Ma for providing purified Src kinase, Esin Kutluay for discussions on experiments, and Eduardo Torres for critical discussions and assistance with preparation of figures. B. A. gratefully acknowledges support from the U.S. Army Breast Cancer Program. This work was supported by grants from the National Institutes of Health (to X. -Y. H.) and the National Science Foundation, Arnold and Mabel Beckman Foundation, and Sidney Kimmel Foundation for Cancer Research (to M. K. R).

Received June 21, 2000; revised July 11, 2000.

References

Abe, K.I.P., W., O'Bryan, J.P., and Der, C.J. (1999). Involvement of NH(2)-terminal sequences in the negative regulation of Vav signaling and transforming activity. J. Biol. Chem. *274*, 30410–30418.

Aghazadeh, B., Liu, G.A., Zhu, K., Zhang, Y., and Rosen, M.K. (1998). Structure and Mutagenesis of the Dbl Homology Domain. Nat. Struct. Biol. *5*, 1098–1107.

Ambruso, D.R., Knall, C., Abell, A.N., Panepinto, J., Kurkchubasche, A., Thurman, G., Gonzalez-Aller, C., Hiester, A., deBoer, M., Harbeck, R.J., et al. (2000). Human neutrophil immunodeficiency syndrome is associated with an inhibitory Rac2 mutation. Proc. Natl. Acad. Sci. *97*, 4654–4659.

Billuart, P., Bienvenu, T., Ronce, N. des Portes, V., Vinet, M.C., Zemni, R., Crollius, H.R., Carrie, A., Fauchereau, F., Cherry, M., et al. (1998). Oligophrenin-1 encodes a rhoGAP protein involved in X-linked mental retardation. Nature *392*, 923–926.

Boguski, M., and McCormick, F. (1993). Proteins regulating Ras and its relatives. Nature *366*, 643–654.

Bourne, H.R., Sanders, D.A., and McCormick, F. (1991). The GTPase superfamily: conserved structure and molecular mechanism. Nature *349*, 117–127.

Brunati, A.M., Donella-Deana, A., Ruzzene, M., Marin, O., and Pinna, L.A. (1995). Site specificity of p72syk protein tyrosine kinase: efficient phosphorylation of motifs recognized by Src homology 2 domains of the Src family. FEBS Lett. *367*, 149–152.

Brunger, A.T., Adams, P.D., Clore, G.M., DeLano, W.L., Gros, P., Grosse-Kunstleve, R.W., Jiang, J.S., Kuszewski, J., Nilges, M., Pannu, N.S., et al. (1998). Crystallography & NMR system: A new software suite for macromolecular structure determination. Acta Crystallogr. D Biol. Crystallogr. *54*, 905–921.

Bustelo, X.R. (1996). The VAV family of signal transduction molecules. Crit. Rev. Oncog. *7*, 65–88.

Bustelo, X.R., and Barbacid, M. (1992). Tyrosine phosphorylation of the vav proto-oncogene product in activated B cells. Science *256*, 1196–1199.

Bustelo, X.R., Ledbetter, J.A., and Barbacid, M. (1992). Product of vav proto-oncogene defines a new class of tyrosine protein kinase substrates. Nature *356*, 68–71.

Carson, M.J. (1991). Ribbons 2.0. J. Appl. Crystallogr. *24*, 958–961.

Cerione, R.A., and Zheng, Y. (1996). The Dbl family of oncogenes. Curr. Opin. Cell. Biol. *8*, 216–222.

Chen, Y.R., and Tan, T.H. (2000). The c-Jun N-terminal kinase pathway and apoptotic signaling. Int. J. Oncol. *16*, 651–662.

Cornilescu, G., Delaglio, F., and Bax, A. (1999). Protein backbone angle restraints from searching a database for chemical shift and sequence homology. J. Biomol. NMR *13*, 289–302.

Crespo, P., Bustelo, X.R., Aaronson, D.S., Coso, O.A., Lopez-Barahona, M., Barbacid, M., and Gutkind, J.S. (1996). Rac-1 dependent stimulation of the JNK/SAPK signaling pathway by Vav. Oncogene *13*, 455–460.

Crespo, P., Schuebel, K.E., Ostrom, A.A., Gutkind, J.S., and Bustelo, X.R. (1997). Phosphotyrosine-dependent activation of Rac-1 GDP/GTP exchange by the vav proto-oncogene product. Nature *385*, 169–172.

Das, B., Shu, X., Day, G.J., Han, J., Krishna, U.M., Falck, J.R., and Broek, D. (2000). Control of intramolecular interactions between the pleckstrin homology and dbl homology domains of vav and sos1 regulates rac binding. J. Biol. Chem. *275*, 15074–15081.

Deckert, M., Tartare-Deckert, S., Couture, C., Mustelin, T., and Altman, A. (1996). Functional and physical interactions of Syk family kinases with the Vav proto-oncogene product. Immunity *5*, 591–604.

Delaglio, F., Grzesiek, S., Vuister, G.W., Zhu, G., Pfeifer, J., and Bax, A. (1995). NMRPipe: a multidimensional spectral processing system based on UNIX pipes. J. Biomol. NMR *6*, 277–293.

Downward, J. (1996). Control of ras activation. Cancer. Surv. *27*, 87–100.

Fischer, K.D., Kong, Y.Y., Nishina, H., Tedford, K., Marengere, L.E., Kozieradzki, I., Sasaki, T., Starr, M., Chan, G., Gardener, S., et al.

(1998). Vav is a regulator of cytoskeletal reorganization mediated by the T- cell receptor. Curr. Biol. *8*, 554–562.

Fischer, K.D., Zmuldzinas, A., Gardner, S., Barbacid, M., Bernstein, A., and Guidos, C. (1995). Defective T-cell receptor signalling and positive selection of Vav-deficient CD4+ CD8+ thymocytes. Nature *374*, 474–477.

Fleming, I.N., Elliott, C.M., Buchanan, F.G., Downes, C.P., and Exton, J.H. (1999). Ca2+/calmodulin-dependent protein kinase II regulates Tiam1 by reversible protein phosphorylation. J. Biol. Chem. *274*, 12753–12758.

Gardner, K., and Kay, L. (1997). Production and incorporation of ^{15}N, ^{13}C, $^{2}H(^{1}H$-1 methyl) isoleucine into proteins for multidimensional NMR studies. J. Am. Chem. Soc. *119*, 7599–7600.

Gardner, K., Konrat, R., Rosen, M., and Kay, L. (1996). A (H)C(CO)NH-TOCSY pulse scheme for sequential assignment of protonated methyl groups in otherwise deuterated ^{15}N, ^{13}C labeled proteins. J. Biomol. NMR *8*, 351–356.

Hall, A. (1998). Rho GTPases and the actin cytoskeleton. Science *279*, 509–514.

Han, J., Das, B., Wei, W., Van Aelst, L., Mosteller, R.D., Khosravi-Far, R., Der Westwick, J.K., and Broek, D. (1997). Lck regulates Vav activation of members of the Rho family of GTPases. Mol. Cell. Biol. *17*, 1346–1353.

Han, J., Luby-Phelps, K., Das, B., Shu, X., Xia, Y., Mosteller, R.D., Krishna, U.M., Falck, J.R., White, M.A., and Broek, D. (1998). Role of substrates and products of PI 3-kinase in regulating activation of Rac-related guanosine triphosphatases by Vav. Science *279*, 558–560.

Holsinger, L.J., Graef, I.A., Swat, W., Chi, T., Bautista, D.M., Davidson, L., Lewis, R.S., Alt, F.W., and Crabtree, G.R. (1998). Defects in actin-cap formation in Vav-deficient mice implicate an actin requirement for lymphocyte signal transduction. Curr. Biol. *8*, 563–572.

Johnson, B.A., and Blevins, R.A. (1994). NMRView: a computer program for the visualization and analysis of NMR data. J. Biomol. NMR *4*, 603–614.

Kay, L.E., Clore, G.M., Bax, A. and Gronenborn, A.M. (1990). Four-dimensional heteronuclear triple-resonance NMR spectroscopy of interleukin-1b in solution. Science *249*, 411–414.

Kay, L.E., Xu, G.Y., Singer, A.U., Muhandiram, D.R., and Forman-Kay, J.D. (1993). A gradient-enhanced HCCH-TOCSY experiment for recording side-chain proton and carbon-13 correlations in water samples of proteins. J. Magn. Reson. Ser. B *101*, 333–337.

Kay, L.E., Yi., X.G., and Yamazaki, T. (1994). Enhanced-sensitivity triple-resonance spectroscopy with minimal H_2O saturation. J. Magn. Reson. Ser. A *109*, 129–133.

Kiyono, M., Kaziro, Y., and Satoh, T. (2000). Induction of rac-guanine nucleotide exchange activity of Ras-GRF1/CDC25(Mm) following phosphorylation by the nonreceptor tyrosine kinase Src. J. Biol. Chem. *275*, 5441–5446.

Laskowski, R.A., Rullmannn, J.A., MacArthur, M.W., Kaptein, R., and Thornton, J.M. (1996). AQUA and PROCHECK-NMR: programs for checking the quality of protein structures solved by NMR. J. Biomol. NMR *8*, 477–486.

Liu, X., Wang, H., Eberstadt, M., Schnuchel, A., Olejniczak, D.T., Meadows, R.P., Schkeryantz, J.M., Janowich, D.A., Harlan, J.E., Harris, E.A.S., et al. (1998). NMR structure and mutagenesis of the N-terminal Dbl homology domain of the nucleotide exchange factor trio. Cell *95*, 269–277.

Logan, T.M., Olejniczak, E.T., Xu, R.X., and Fesik, S.W. (1993). A general method for assigning NMR spectra of denatured proteins using 3D HC(CO)NH-TOCSY triple resonance experiments. J. Biomol. NMR *3*, 225–231.

Lopez-Lago, M., Lee, H., Cruz, C., Movilla, N., and Bustelo, X.R. (2000). Tyrosine phosphorylation mediates both activation and downmodulation of the biological activity of Vav. Mol. Cell. Biol. *20*, 1678–1691.

Margolis, B., Hu, P., Katzav, S., Li, W., Oliver, J.M., Ullrich, A., Weiss, A., and Schlessinger, J. (1995). Tyrosine phosphorylation of vav proto-oncogene product containing SH2 domain and transcription factor motifs. Nature *356*, 71–74.

Matsuo, H., Kupce, E., Li, H., and Wagner, G. (1996). Use of selective C alpha pulses for improvement of HN(CA)CO-D and HN(COCA)NH-D experiments. J. Magn. Reson. Ser. B *111*, 194–198.

Michiels, F., Habets, G.G., Stam, J.C., van der Kammen, R.A., and Collard, J.G. (1995). A role for Rac in Tiam1-induced membrane ruffling and invasion. Nature *375*, 338–340.

Muhandiram, D.R., and Kay, L.E. (1994). Gradient-enhanced triple-resonance three-dimensional NMR experiments with improved sensitivity. J. Magn. Reson. Ser. B *103*, 203–216.

Neri, D., Szyperski, T., Otting, G., Senn, H., and Wuthrich, K. (1989). Stereospecific nuclear magnetic resonance assignments of the methyl groups of valine and leucine in the DNA-binding domain of the 434 repressor by biosynthetically directed fractional ^{13}C labeling. Biochemistry *28*, 7510–7516.

Nicholls, A., Sharp, K.A., and Honig, B. (1991). Protein folding and association: insights from the interfacial and thermodynamic properties of hydrocarbons. Struct. Funct. Genet. *11*, 281–296.

Nilges, M., Macias, M.J., O'Donoghue, S.I., and Oschkinat, H. (1997). Automated NOESY interpretation with ambiguous distance restraints: the refined NMR solution structure of the pleckstrin homology domain from beta-spectrin. J. Mol. Biol. *269*, 408–422.

Nomanbhoy, T., Leonard, D., Manor, D., and Cerione, R. (1996). Investigation of the GTP-binding/GTPase cycle of Cdc42Hs using extrinsic reporter group fluorescence. Biochemistry *35*, 4602.

Pasteris, N.G., Cadle, A., Logie, L.J., Proteous, M.E.M., Schwartz, C.E., Stevenson, R.E., Glover, T.W., Wilroy, R.S., and Gorski, J.L. (1994). Isolation and characterization of the faciogenital dysplasia (Aarskog-Scott syndrome) gene: a putative Rho/Rac guanine nucleotide exchange factor. Cell *79*, 669–678.

Qiu, R.G., Chen, J., Kirn, D., McCormick, F., and Symons, M. (1995). An essential role for Rac in Ras transformation. Nature *374*, 457–459.

Schuebel, K.E., Movilla, N., Rosa, J.L., and Bustelo, X.R. (1998). Phosphorylation-dependent and constitutive activation of Rho proteins by wild-type and oncogenic Vav-2. EMBO J. *17*, 6608–6621.

Soisson, S.M., Nimnual, A.S., Uy, M., Bar-Sagi, D., and Kuriyan, J. (1998). Crystal structure of the Dbl and pleckstrin homology domains from the human son of sevenless protein. Cell *95*, 259–268.

Songyang, Z., Shoelson, S.E., Chaudhuri, M., Gish, G., Pawson, T., Haser, W.G., King, F., Roberts, T., Ratnofsky, S., Lechleider, R.J., et al. (1993). SH2 domains recognize specific phosphopeptide sequences. Cell *72*, 767–778.

Szilak, L., Moitra, J., Krylov, D., and Vinson, C. (1997). Phosphorylation destabilizes alpha-helices. Nat. Struct. Biol. *4*, 112–114.

Tarakhovsky, A., Turner, M., Schaal, S., Mee, P.J., Duddy, L.P., Rajewsky, K., and Tybulewicz, V.L. (1995). Defective antigen receptor-mediated proliferation of B and T cells in the absence of Vav. Nature *374*, 467–470.

Thomas, S.M., and Brugge, J.S. (1997). Cellular functions regulated by Src family kinases. Annu. Rev. Cell. Dev. Biol. *13*, 513–609.

Wishart, D.S., and Sykes, B.D. (1994). The ^{13}C chemical-shift index: a simple method for the identification of protein secondary structure using ^{13}C chemical-shift data. J. Biomol. NMR *4*, 171–180.

Wuthrich, K. (1986). NMR of proteins and nucleic acids (New York: John Wiley & Sons).

Zhang, R., Alt, F.W., Davidson, L., Orkin, S.H., and Swat, W. (1995). Defective signalling through the T- and B-cell antigen receptors in lymphoid cells lacking the vav proto-oncogene. Nature *374*, 470–473.

Zhu, K., Debreceni, B., Li, R., and Zheng, Y. (2000). Identification of Rho GTPase-dependent sites in the DH domain of oncogenic Dbl that are required for transformation. J. Biol. Chem., in press.

Zwahlen, C., Vincent, S.J.F., Gardner, K.H., and Kay, L.E. (1998). Significantly improved resolution for NOE correlations from valine and isoleucine (Cg2) methyl groups in ^{15}N,^{13}C- and ^{15}N, ^{13}C, ^{2}H-labeled proteins. J. Am. Chem. Soc. *120*, 4825–4831.

Protein Data Bank ID Code

Coordinates of 20 NMR derived structures have been deposited in the RCSB Protein Data Bank with ID code 1F5X.